

Welcome to the Multi-Messenger Era!

Lessons from a Neutron Star Merger and the Landscape Ahead

Brian D. Metzger
 Columbia Astrophysics Laboratory
 Columbia University
 bmetzger@phys.columbia.edu

October 18, 2017

Abstract

The discovery by Advanced LIGO/Virgo of gravitational waves from the binary neutron star merger GW170817, and subsequently by astronomers of transient counterparts across the electromagnetic spectrum, has initiated the era of “multi-messenger astronomy”. Given the slew of papers appearing on this event, I thought it useful to summarize the electromagnetic discoveries in the context of theoretical counterpart models and to present personal views on the major take-away lessons and outstanding new questions from this watershed event. The weak burst of gamma-rays discovered in close time coincidence with GW170817, and potential evidence for a more powerful off-axis relativistic jet (initially beamed away from our line of sight) via the delayed rise of a non-thermal X-ray and radio orphan afterglow, provides the most compelling evidence yet that cosmological short gamma-ray bursts originate from binary NS mergers. The luminosity and colors of the early optical emission discovered within a day of the merger agrees strikingly well with original predictions of Metzger et al. (2010) for “kilonova” emission powered by the radioactive decay of r -process nuclei, the binary NS merger origin of which was initially proposed by Lattimer & Schramm (1974). The transition of the spectral energy distribution to near-infrared wavelengths on timescales of days matches the predictions by Barnes & Kasen (2013) and Tanaka & Hotokezaka (2013) if a portion of the ejecta contains heavy r -process nuclei with higher opacities due to the presence of lanthanides. The “blue” and “red” ejecta components may possess distinct origins (e.g. dynamical ejecta versus accretion disk outflows), with key implications for the physics of the merger and the properties of neutron stars. I outline the diversity in the counterpart emission expected from additional mergers—observed with a range of different binary masses and viewing angles—discovered in the years ahead as LIGO/Virgo approach design sensitivity and NS mergers are discovered as frequently as once per week.

1 A Big Reveal from the Cosmos

When a neutron star (NS) binary coalesces into a single object following a prolonged inspiral driven by gravitational wave (GW) radiation, the outcome is a prodigious collision which releases mass and energy into the surrounding environment on a timescale as short as milliseconds. The merger aftermath was predicted to be accompanied by a diverse range of thermal and non-thermal electromagnetic (EM) counterparts from radio to gamma-ray frequencies (e.g. Bloom et al. 2009; Metzger & Berger 2012; Piran et al. 2013; Rosswog 2015; Fernández & Metzger 2016). The discovery of the first GW chirp from a binary NS merger GW170817 by the Advanced LIGO and Virgo collaboration (LIGO Scientific Collaboration & Virgo Collaboration, 2017a), and its subsequent localization to a host galaxy at a distance of only ≈ 40 Mpc (e.g. LIGO Scientific Collaboration et al. (2017a) and references therein), provided astronomers with a golden opportunity to test theoretical predictions for the EM and nucleosynthetic signatures of these events, as established by the work of astrophysicists over the last 40 years.

The discovery and announcement of GW170817 was followed by the most ambitious (and emotionally charged) campaign of EM follow-up observations ever conducted (LIGO Scientific Collaboration et al., 2017a). Observations covered the gamut of frequencies, including radio/microwave (e.g. Mooley et al. 2017; Murphy et al. 2017; Hallinan et al. 2017; Alexander et al. 2017), infrared (e.g. Chornock et al. 2017; Levan & Tanvir 2017; Kasliwal et al. 2017), optical/UV (e.g. Coulter et al. 2017; Allam et al. 2017; Yang et al. 2017; Arcavi et al. 2017a; Kilpatrick et al. 2017; McCully et al. 2017; Pian et al. 2017; Arcavi et al. 2017b; Tanvir & Levan 2017; Evans et al. 2017; Lipunov et al. 2017; Cowperthwaite et al. 2017;

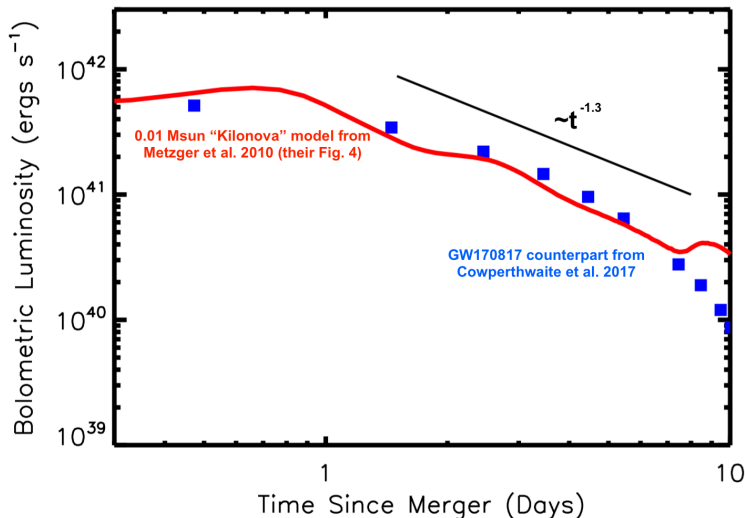


Figure 1: Bolometric light curve of the optical/infrared counterpart of GW170817 (blue squares) from multi-band photometry (Cowperthwaite et al., 2017) compared to the fiducial model of Metzger et al. (2010) (red line; their Fig. 4) for “kilonova” emission powered by the radioactive decay of $10^{-2} M_{\odot}$ of r -process matter expanding at $v = 0.1 c$, assuming complete thermalization of the radioactive decay products. Shown above for comparison is a line with the approximate power-law decay $\propto t^{-1.3}$ for r -process heating (Metzger et al., 2010; Hotokezaka et al., 2017). The true ejecta mass required to explain the data exceeds $0.01 M_{\odot}$ by a factor of several (Table 1) because the actual thermalization efficiency is less than unity (Barnes et al., 2016; Rosswog et al., 2017). The observed color evolution of the transient from optical to near-infrared wavelengths can also only be understood by accounting for the details of the ejecta structure and the different opacities of light and heavy r -process nuclei (§2.2 for details).

Smartt et al. 2017; Shappee et al. 2017), X-ray (Troja et al., 2017; Margutti et al., 2017; Haggard et al., 2017; Fong et al., 2017), gamma-ray (e.g. Goldstein et al. 2017; Savchenko et al. 2017; LIGO Scientific Collaboration et al. 2017b; Verrechia et al. 2017), and even neutrinos (ANTARES et al. 2017). The full range of observational references are summarized in LIGO Scientific Collaboration et al. (2017a).

Often in astronomy, hints of the underlying truth about a phenomenon build up only gradually as the capabilities of telescopes incrementally improve; and even once a consensus opinion is reached, it is often the product of several pieces of indirect evidence. GW170817 represents a sharp departure from this rule, as LIGO/Virgo transported us, in one quantum leap, directly from the dark into the light (the “Big Reveal”), albeit a leap that theorists had long anticipated and given unusually extensive consideration to, despite the lack of observational guidance. As information on the discovery percolated in, I was overtaken by the degree to which the optical and infrared transient being observed agreed with those predicted by myself and colleagues, such as work I led in 2010 (Fig. 1). Seeing Nature agree so well with our basic ideas is a triumph for astrophysics theory.

Given the slew of observational and interpretation papers appearing on this topic over just a few days, I thought it useful to review briefly, in one place, theoretical models for the EM counterparts of binary NS mergers in the context of the GW170817 discovery. I start by describing the thermal kilonova emission coming from the mildly-relativistic merger ejecta (§2) and then discuss non-thermal emission from the ultra-relativistic gamma-ray burst (GRB) jet (§3). Figure 2 summarizes a reasonable guess for the origin of the different EM counterparts observed following GW170817. In §4, I draw major take-away lessons from the first binary NS merger, and use them to motivate new questions for scrutiny as the sample of EM/GW events grows over the next several years. Many of the interpretations presented result from interaction with the observational groups in which I collaborated, particularly the Dark Energy Camera (DECam) group, and I encourage the reader to consult these works for in-depth analysis of these data.

2 Kilonovae and the Origin of the Heaviest Elements

The optical/infrared transient following GW170817 is fully consistent with being powered by the radioactive decay of nuclei synthesized in the NS merger ejecta. Here, I review the history of models for the r -process in binary NS mergers and the expected sources of mass ejection in these events based on numerical simulations (§2.1). I then describe the historical development of kilonova models (§2.2) in the context of their expected timescales, luminosities and colors; particular emphasis is placed on the distinction between the emission from ejecta containing light versus heavy r -process nuclei. Within this framework, in §2.3 I summarize our interpretation for the kilonova from GW170817, and the resulting implications for the fate of the merger remnant and the properties of NSs more broadly.

2.1 Mass Ejection in Binary NS Mergers and the r -Process

Roughly 60 years ago, Burbidge et al. (1957) and Cameron (1957) recognized that approximately half of the elements in the Galaxy heavier than iron must have been produced in an environment in which

Table 1: Key Properties of GW170817

Property	Value	Reference
Chirp mass, \mathcal{M} (rest frame)	$1.188^{+0.004}_{-0.002} M_{\odot}$	1
First NS mass, M_1	$1.36 - 1.60 M_{\odot}$ (90%, low spin prior)	1
Second NS mass, M_2	$1.17 - 1.36 M_{\odot}$ (90%, low spin prior)	1
Total binary mass, $M_{\text{tot}} = M_1 + M_2$	$\approx 2.74^{+0.04}_{-0.01} M_{\odot}$	1
Observer angle relative to binary axis, θ_{obs}	$11 - 33^{\circ}$ (68.3%)	2
Blue KN ejecta ($A_{\text{max}} \lesssim 140$)	$\approx 0.01 - 0.02 M_{\odot}$	e.g., 3,4,5
Red KN ejecta ($A_{\text{max}} \gtrsim 140$)	$\approx 0.04 M_{\odot}$	e.g., 3,5,6
Light r -process yield ($A \lesssim 140$)	$\approx 0.05 - 0.06 M_{\odot}$	
Heavy r -process yield ($A \gtrsim 140$)	$\approx 0.01 M_{\odot}$	
Gold yield	$\sim 100 - 200 M_{\oplus}$	8
Uranium yield	$\sim 30 - 60 M_{\oplus}$	8
Kinetic energy of off-axis GRB jet	$10^{49} - 10^{50}$ erg	e.g., 9, 10, 11, 12
ISM density	$10^{-4} - 10^{-2} \text{ cm}^{-3}$	e.g., 9, 10, 11, 12

(1) LIGO Scientific Collaboration et al. 2017c; (2) depends on Hubble Constant, LIGO Scientific Collaboration et al. 2017d; (3) Cowperthwaite et al. 2017; (4) Nicholl et al. 2017; (5) Kasen et al. 2017; (6) Chornock et al. 2017; (8) assuming heavy r -process ($A > 140$) yields distributed as solar abundances (Arnoult et al., 2007); (9) Margutti et al. 2017; (10) Troja et al. 2017; (11) Fong et al. 2017; (12) Hallinan et al. 2017

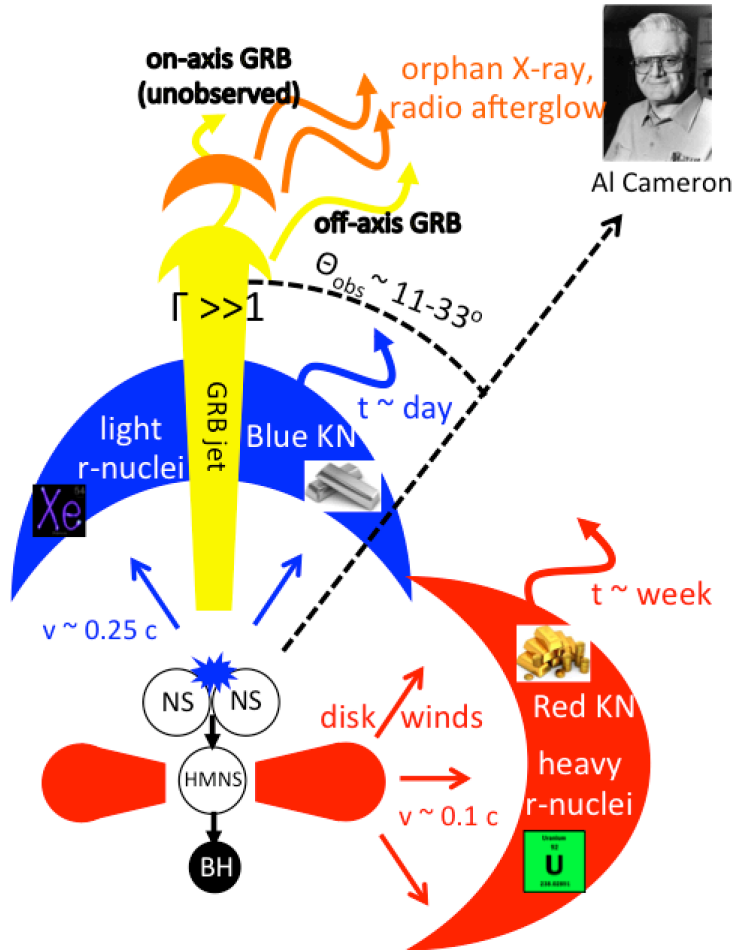


Figure 2: Scenario for the EM counterparts of GW170817, as viewed by the observer (Al Cameron) from the inferred binary inclination angle $\theta_{\text{obs}} \approx 0.2 - 0.5$ (LIGO Scientific Collaboration et al., 2017d), as motivated by interpretations presented in several papers (e.g. Cowperthwaite et al. 2017; Kasen et al. 2017; Nicholl et al. 2017; Chornock et al. 2017; Fong et al. 2017; Kasen et al. 2017; Margutti et al. 2017; LIGO Scientific Collaboration et al. 2017b). **Timeline:** (1) Two NSs with small radii $\lesssim 11$ km and comparable masses ($q \approx 1$) coalesce. The dynamical stage of the merger ejects only a small mass $\lesssim 10^{-2} M_{\odot}$ in equatorial tidal ejecta, but a larger quantity $\approx 10^{-2} M_{\odot}$ of $Y_e > 0.25$ matter into the polar region at $v \approx 0.2 - 0.3 c$, which synthesizes exclusively light r -process nuclei (e.g. xenon and silver); (2) The merger product is a meta-stable hypermassive NS, which generates a large accretion torus $\sim 0.1 M_{\odot}$ as it sheds its angular momentum and collapses into a BH on a timescale of $\lesssim 100$ ms; (3) The torus-BH powers a collimated GRB jet, which burrows through the polar dynamical ejecta on a timescale of $\lesssim 2$ s; (4) Gamma-rays from the core of the GRB jet are relativistically beamed away from our sight line, but a weaker GRB is nevertheless observed from the off-axis jet or the hot cocoon created as the jet breaks through the polar ejecta; (5) On a similar timescale, the accretion disk produces a powerful wind ejecting $\approx 0.04 M_{\odot}$ of $Y_e \lesssim 0.25$ matter which expands quasi-spherically at $v \approx 0.1 c$ and synthesizes also heavy r -process nuclei such as gold and uranium; (6) After several hours of expansion, the polar ejecta becomes diffusive, powering \sim visual wavelength (“blue”) kilonova emission lasting for a few days; (7) over a longer timescale ≈ 1 week, the deeper disk wind ejecta becomes diffusive, powering red kilonova emission; (8) the initially on-axis GRB jet decelerates by shocking the ISM, such that after ≈ 2 weeks its X-ray and radio synchrotron afterglow emission rises after entering the observer’s causal cone.

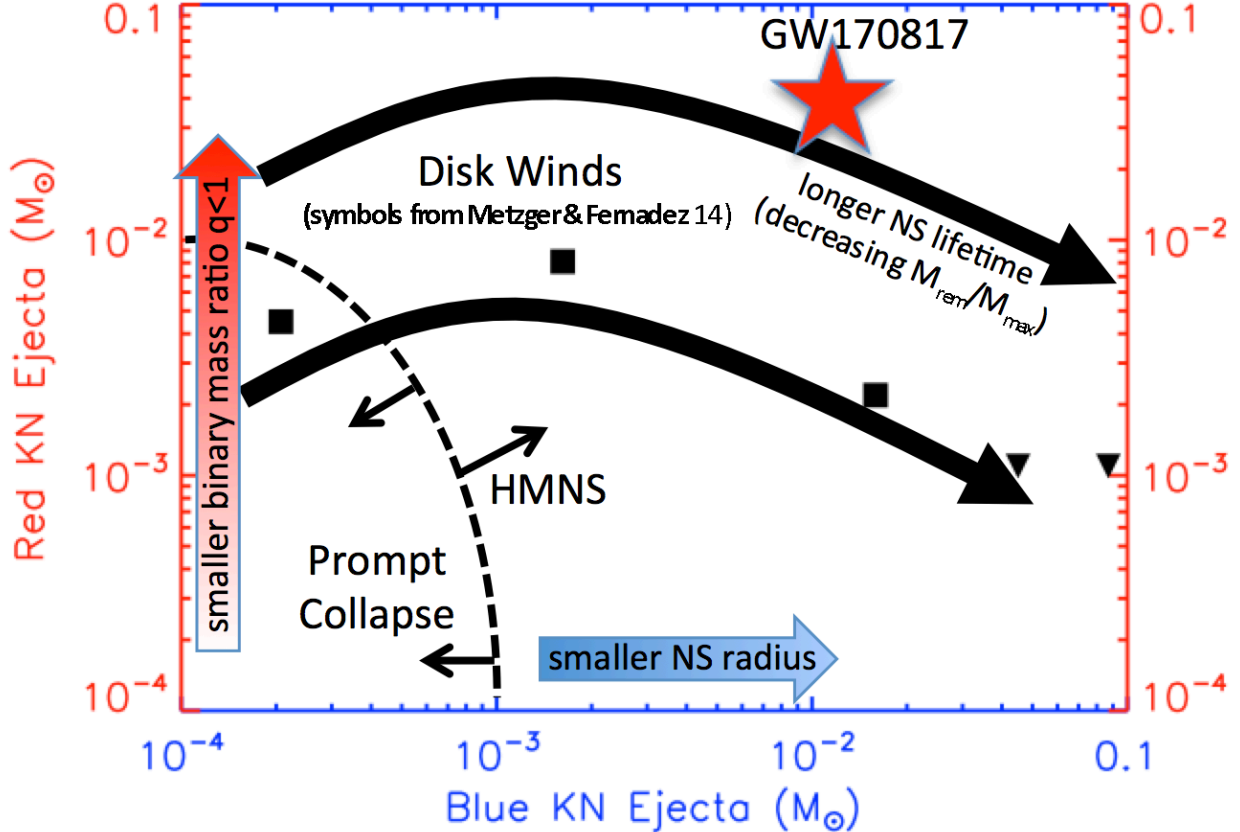


Figure 3: Quantity of lanthanide-free (light r -process; “blue KN”) ejecta and lanthanide-bearing (heavy r -process; “red KN”) ejecta from a binary NS merger and its dependence on the properties of the binary (remnant mass M_{rem} , NS radius, and maximum mass NS M_{max}) in comparison to those inferred from the blue and red kilonova emission of GW170817 (e.g. Cowperthwaite et al. 2017; Nicholl et al. 2017; Chornock et al. 2017). The amount of low- Y_e (red) tidal tail ejecta increases for more asymmetric binaries (decreasing binary mass ratio $q = M_2/M_1 < 1$), while the amount of high- Y_e (blue) shock-heated ejecta ejected dynamically into the polar regions is larger if the colliding NSs possess smaller radii. For a massive binary with a high ratio of $M_{\text{rem}}/M_{\text{max}}$, the merger product promptly collapses to a BH, producing little blue shock-heated ejecta. The dependence of the disk wind ejecta composition, as approximately delineated as the region between the black arrows, is more complex and depends on the lifetime of the hyper- or supra-massive NS merger remnant, which increases with decreasing $M_{\text{rem}}/M_{\text{max}}$ (Metzger & Fernández 2014; Perego et al. 2014; Kasen et al. 2015).

the density of free neutrons was so high that neutron captures on nuclei proceed much faster than β -decays. Since that time, however, while the astrophysical sites of most of the other nucleosynthesis channels identified in these pioneering works have been identified, the origin of the rapid neutron capture process (“ r -process”, for short) has remained an enduring mystery. Hot outflows from the newly-formed proto-neutron stars created in core collapse supernovae were at one time considered the most promising contender. However, this model is known to exhibit large theoretical difficulties (e.g. Qian & Woosley 1996), and several lines of evidence in recent years have pointed towards an r -process source which is much rarer than standard supernovae (Wallner et al., 2015; Hotokezaka et al., 2015; Ji et al., 2016; Macias & Ramirez-Ruiz, 2016)

Lattimer & Schramm (1974) proposed that the coalescence of a binary system consisting of a NS and a stellar mass black hole (BH) would provide a promising source of neutron-rich ejecta conducive to the r -process with a very low electron fraction $Y_e = n_p/(n_n + n_p)$, where n_p and n_n are the densities of protons and neutrons, respectively. Following the ejection of NS matter through the outer binary Lagrange points by tidal forces, its rapid decompression from nuclear densities would naturally result in the formation of heavy nuclei through neutron capture (Lattimer et al., 1977; Meyer, 1989). Symbalisty & Schramm (1982) and Eichler et al. (1989) proposed that a similar mechanism of mass ejection could occur from merging compact binaries consisting of two NSs. The first numerical simulations of binary NS mergers showing tidal mass ejection followed (Davies et al. 1994; Ruffert et al. 1997; Rosswog et al. 1999), with subsequent work establishing that the r -process of this extremely neutron-rich matter ($Y_e \lesssim 0.1 - 0.2$) would result

Table 2: Sources of r -Process Ejecta in Binary Neutron Star Mergers

Ejecta Type	$M_{\text{ej}}(M_{\odot})$	$v_{\text{ej}}(c)$	Color	M_{ej} decreases with	References
Tidal Tails	$\sim 10^{-4} - 10^{-2}$	$0.15 - 0.35$	Red (NIR)	$q = M_2/M_1$	e.g., 1,2
Polar Shocked	$\sim 10^{-4} - 10^{-2}$	$0.15 - 0.35$	Blue (visual)	$M_{\text{rem}}/M_{\text{max}}, R_{\text{ns}}$	e.g., 3–5
Disk Outflows	$10^{-4} - 0.07$	$0.03 - 0.1$	Blue+Red	$M_{\text{rem}}/M_{\text{max}}$	e.g., 6–8

(1) Rosswog et al. 1999; (2) Hotokezaka et al. 2013; (3) Bauswein et al. 2013; (4) Sekiguchi et al. 2016; (5) Radice et al. 2016; (6) Fernández & Metzger 2013; (7) Perego et al. 2014; (8) Just et al. 2015; (9) Siegel & Metzger 2017

in an heavy element abundance pattern broadly consistent with that in the solar system (Freiburghaus et al., 1999; Goriely et al., 2011). Tidally-ejected matter expands away from the merger site primarily in the equatorial plane of the binary at velocities $\sim 0.2 - 0.3$ c, and its quantity $\sim 10^{-4} - 10^{-2}M_{\odot}$ is a sensitive decreasing function of the binary mass ratio $q = M_2/M_1 < 1$ (e.g. Rosswog et al. 1999; Hotokezaka et al. 2013), i.e. more asymmetric mergers eject greater mass tidally.

In addition to the tidal ejecta, contemporary numerical simulations have established a separate ejecta source originating from the interface between the merging stars and emerging into the high latitude polar region (Oechslin & Janka, 2006; Hotokezaka et al., 2013; Bauswein et al., 2013). Heating due to shocks and neutrino-irradiation promote weak interactions (e.g. $n\nu_e \rightarrow pe^-$, $e^+n \rightarrow p\bar{\nu}_e$) which raise the electron fraction of the polar ejecta to values $Y_e \gtrsim 0.25$ well above its initial composition in the neutron star interior (Wanajo et al., 2014; Goriely et al., 2015; Sekiguchi et al., 2016; Radice et al., 2016). Though relatively independent of the binary mass ratio, the quantity of shock-heated polar ejecta instead depends sensitively on the NS radius (see below) and the lifetime of the compact remnant created during the merger. If the baryonic mass of the binary (and thus of its compact central remnant, M_{rem}) exceeds the maximum mass of a neutron star, M_{max} , by a factor of $f = 1.3 - 1.6$ (the precise value depending on the EOS; Bauswein et al. 2013b), then the merger product promptly collapses to a BH with little or no polar dynamical ejecta (Shibata & Taniguchi, 2006). On the other hand, if $M_{\text{rem}} \lesssim fM_{\text{max}}$ then the merger product is a hyper- or supra-massive NS, which is at least temporarily stable to collapse due to its rapid rotation. The quantity of polar dynamical ejecta in this case exceeds the prompt collapse case, varying from $\sim 10^{-3} - 10^{-2}M_{\odot}$, depending most sensitively on the radii of the NSs; a more compact NS results in the collision occurring deeper in the gravitational potential and thus produces stronger shock-heating and greater mass loss (e.g. Bauswein et al. 2013).

Debris from the merger which is not immediately unbound can possess enough angular momentum to circularize into an accretion disk around the central remnant, providing an agent to power an ultra-relativistic GRB jet (e.g. Narayan et al. 1992; §3). Slower expanding outflows from this remnant disk, which occur on timescales of up to seconds post merger, provide another important source of r -process ejecta (e.g. Metzger, Piro & Quataert 2008; Dessart et al. 2009). The quantity of mass in the disk outflows $M_{\text{ej}}^{\text{disk}}$ scales approximately with the original mass of the torus M_t , with $M_{\text{ej}}^{\text{disk}} \approx 0.2 - 0.4M_t$ (Fernández & Metzger, 2013; Perego et al., 2014; Just et al., 2015; Fernández et al., 2015; Siegel & Metzger, 2017). Because the mass of the torus increases with both the mass ratio of the binary and the lifetime of the hypermassive NS (e.g. Hotokezaka et al. 2013), $M_{\text{ej}}^{\text{disk}}$ is also an decreasing function of q and $M_{\text{rem}}/M_{\text{max}}$, i.e. an asymmetric merger or long-lived NS remnant produces a greater quantity of disk ejecta. For a massive torus $\gtrsim 0.1 - 0.2M_{\odot}$ the disk ejecta mass $M_{\text{ej}}^{\text{disk}} \sim 0.05 - 0.1M_{\odot}$ can greatly exceed that of the dynamical ejecta. The electron fraction distribution of the disk outflows, though generally broad $Y_e \sim 0.1 - 0.4$ (Just et al., 2015), depends on the lifetime of the central neutron star remnant due to the de-neutronizing impact of its strong electron neutrino luminosity. The average Y_e of the disk outflow grows with the time the hyper- or supra-massive NS survives before collapsing to a BH (Metzger & Fernández 2014; Perego et al. 2014). Disk outflow simulations find that the unbound matter achieves asymptotic speeds $v_{\text{ej}} \approx 0.03 - 0.1$ c which are typically 2 – 3 times lower than the velocity of the dynamical ejecta.

Figure 3 and Table 2 summarizes the quantity of lanthanide-poor (“blue”) and lanthanide-rich (“red”) ejecta from neutron star mergers from both dynamical and disk wind channels, and their dependence on properties of the binary (remnant mass M_{rem} , mass ratio) and neutron star (radius, maximum M_{max}). The disk wind ejecta exhibits a complex behavior with increasing remnant lifetime (decreasing $M_{\text{rem}}/M_{\text{max}}$), as outlined schematically by the region between the black solid arrows.

2.2 Kilonova Emission Models

Table 3 summarizes the historical progression of kilonova models and their predictions for the luminosity, timescale, and color of the thermal emission. Although models capable of explaining the detailed color

Table 3: Historical Development of Kilonova Models

Model	Opacity Source	L_{peak} (ergs s $^{-1}$)	t_{peak}	SED Peak	Ref.
parameterized heating	e-scattering	$10^{43} - 10^{44}$	~ 1 day	UV	1
r -process heating	iron	$10^{41} - 10^{42}$	~ 1 day	visual	2, 3
La Opacities	heavy r	$10^{40} - 10^{41}$	~ 1 week	NIR	4, 5
“Blue” + “Red”	light + heavy r	$10^{40} - 10^{42}$	1 day \rightarrow 1 week	visual \rightarrow NIR	e.g., 6, 7, 8

(1) Li & Paczyński 1998; (2) Metzger et al. 2010; (3) Roberts et al. 2011; (4) Barnes & Kasen 2013; (5) Tanaka & Hotokezaka 2013; (6) Metzger & Fernández 2014; (7) Martin et al. 2015; (8) Tanaka et al. 2017

evolution of the emission following GW170817 reached their present mature form just in the last couple of years, many of the basic predictions were in place earlier.

Li & Paczyński (1998) first proposed that the radioactive ejecta of a NS merger could power a supernova-like thermal transient. Due to the small quantity of ejecta mass and its high expansion speed ~ 0.1 c, they predicted that the ejecta would become diffusive to photon radiation and the emission would peak on a timescale of $\lesssim 1$ day, much shorter than the rise time of a supernova. However, Li & Paczyński (1998) did not possess a physical model for radioactive heating rate \dot{q} (e.g. based on a nuclear reaction network; the term “ r -process” does not appear in their paper), which they instead parameterized as $\dot{q} \propto t^{-1}$ with the normalization left as a free parameter. Since the peak luminosity is proportional to the heating rate at the time of peak light, their fiducial model reached extremely high values $\sim 10^{44}$ erg s $^{-1}$, close to the brightest supernovae ever discovered, with a spectral peak in the ultra-violet. Such luminous transients following NS merger were disfavored based on observations ruling out their presence following short duration GRBs, after they began to be localized to sufficient accuracy for optical follow-up by the *Swift* satellite starting in 2005 (e.g. Fox et al. 2005; Hjorth et al. 2005; Berger et al. 2005; Bloom et al. 2006).

Metzger et al. (2010) first calculated the late-time radioactive heating from decaying r -process nuclei (predicting $\dot{q} \propto t^{-1.3}$ on timescales of hours to days; Fig. 1), which they incorporated self-consistently into the light curve calculation. They also used a more physical model for the opacity, assuming it was provided by the line (bound-bound) opacity of iron versus the (highly sub-dominant) electron scattering opacity assumed in earlier work. They predicted peak luminosities of $\sim 3 \times 10^{41}$ erg s $^{-1}$ for $10^{-2}M_{\odot}$ of ejecta expanding at $v \sim 0.1$ c and a spectral peak at visual wavelengths. As this was roughly 1000 times more luminous than classical novae (which peak typically close to the Eddington luminosity of $\sim 10^{38}$ erg s $^{-1}$), they dubbed these events “kilonovae.” Metzger & Berger (2012) highlighted that the isotropic nature of the kilonova emission, as compared to the tightly collimated and relativistically beamed GRB/afterglow emission, would make them the most promising counterpart for a typical binary NS merger at 200 Mpc, the range of Advanced LIGO/Virgo at design sensitivity. Kasliwal & Nissanke (2014) emphasized that during the few observing runs with Advanced LIGO, mergers could occur much closer than 200 Mpc and thus kilonovae could be detected even with 1 m class telescopes (as turned out to be the case for GW170817).

Kasen et al. (2013) and Barnes & Kasen (2013) and subsequently, Tanaka & Hotokezaka (2013), performed the first kilonova calculations including line opacity data based on atomic data expected for ejecta containing heavy r -process elements. They showed that if the ejecta contains lanthanide or actinide nuclei with partially-filled f -shell valence electron shells, as occurs if the r -process passes the second abundance peak at atomic mass number $A \approx 130$, then the resulting photon opacity at UV and optical wavelengths is $\gtrsim 10 - 100$ times greater than if the ejecta were composed of iron-like nuclei with partial d -shell valence electrons. This high optical opacity delays the evolution timescale of the light curve from ~ 1 day to ~ 1 week and pushes the spectral peak from visual frequencies predicted by Metzger et al. (2010) and Roberts et al. (2011) to near-infrared wavelengths (Barnes & Kasen, 2013; Tanaka & Hotokezaka, 2013; Grossman et al., 2014; Wollaeger et al., 2017).

Although lanthanide opacities move the kilonova emission to the infrared, **not all portions of the NS merger ejecta necessarily produce such heavy nuclei.** In particular, ejecta with $Y_e \gtrsim 0.25$ lacks sufficient neutrons for neutron-capture reactions to push the nuclear flow past the second r -process peak at $A \approx 130$ (Metzger & Fernández, 2014). In such a case, the lanthanides are not produced, and the ejecta would produce a “blue” and fast-evolving kilonova similar to original expectations (Metzger et al., 2010) because the opacity of light r -process nuclei is only moderately higher than that of iron (Tanaka et al., 2017; Kasen et al., 2017).

At least a small quantity of ejecta with $Y_e \lesssim 0.2$ will be present in any merger from the tidal tail ejecta or disk winds, making “red” kilonova emission a ubiquitous feature. However, outflows from the

accretion disk are more isotropic and thus should expand also into the lanthanide-poor polar regions (Metzger & Fernández, 2014; Perego et al., 2014; Martin et al., 2015), powering a separate component of “blue” emission similar to original kilonova models (Metzger et al., 2010). In original hybrid “blue” + “red” scenarios, the quantity of red versus blue kilonova emission originates from the disk outflows and is diagnostic of the lifetime of the central merger remnant (Fig. 3; Metzger & Fernández 2014; Martin et al. 2015). However, Wanajo et al. (2014) showed that when neutrino transport effects are included, the shock-heated polar dynamical ejecta may also be lanthanide-free with $Y_e \gtrsim 0.25$ (cf. Goriely et al. 2015; Sekiguchi et al. 2016), in which case it could also contribute to—or even dominate—the early-time blue kilonova emission. As depends on the relative velocity of the red and blue ejecta, the blue emission is visible only for viewing angles along which it is not blocked by the higher opacity red matter (e.g. Kasen et al. 2015).

2.3 Interpreting the Kilonova Which Accompanied GW170817

The thermal spectrum of the optical counterpart of GW170817 (e.g. Nicholl et al. 2017; Chornock et al. 2017; Levan & Tanvir 2017) strongly supported the kilonova model, as compared to the power-law spectrum expected for non-thermal GRB afterglow emission. The shape of the bolometric light curve following peak is broadly consistent with the $\propto t^{-1.3}$ radioactive heating rate from freshly synthesized r -process nuclei (Fig. 1; Metzger et al. 2010). Over the first few days the transient colors were blue and rapidly-evolving with a spectral peak at visual wavelengths (e.g. Soares-Santos et al. 2017; Smartt et al. 2017; Troja et al. 2017; Nicholl et al. 2017; Evans et al. 2017; Shappee et al. 2017; Pian et al. 2017; McCully et al. 2017; Cowperthwaite et al. 2017). At later times, the colors became substantially redder and more slowly-evolving on timescales of several days to a week, with a spectral peak around $1.5\mu\text{m}$ (e.g. Chornock et al. 2017; Tanvir & Levan 2017; Pian et al. 2017; Shappee et al. 2017; Kasliwal et al. 2017). The lack of well-defined spectral features is suggestive of line blending due to the photosphere expanding at speeds up to several tenths of the speed of light (Nicholl et al., 2017), though broad undulations in the NIR spectra predicted from lanthanide absorption (Kasen et al., 2013) were possibly observed in GW170817 (e.g. Chornock et al. 2017; Troja et al. 2017). As pointed out by several works (e.g. Kasen et al. 2017; Cowperthwaite et al. 2017; Chornock et al. 2017; Kasliwal et al. 2017; McCully et al. 2017; Smartt et al. 2017; Troja et al. 2017; Pian et al. 2017; Arcavi et al. 2017b), these properties are consistent with the two-component blue+red kilonova picture discussed above (e.g. Metzger & Fernández 2014; ?).

What part of the merger or its aftermath created the ejecta we observe? Both the dynamical merger and the subsequent accretion disk wind can contribute to the ejecta (§2.1, Table 2), making it important to carefully assess the origin of the dominant contribution to the blue and red ejecta components (see Kasen et al. 2017, Cowperthwaite et al. 2017 for a complementary discussion). The quantity of blue (lanthanide-free) ejecta from GW170817 was estimated to be $\approx 1 - 2 \times 10^{-2} M_\odot$ with a mean velocity of $v_{\text{ej}} \approx 0.2 \text{ c}$ (Cowperthwaite et al., 2017; Nicholl et al., 2017), based on fitting the observed light curves to kilonova models (Metzger, 2017) and the spectra to more detailed radiative transfer calculations (Kasen et al., 2017). Comparing these measurements to the results of numerical simulations (§2.1), the high velocity tentatively supports an origin associated with the shock-heated dynamical ejecta (Wanajo et al., 2014; Goriely et al., 2015; Sekiguchi et al., 2016) rather than a disk wind. In such a case, the large *quantity* of the dynamical ejecta would suggest the radii of the merging NSs were relatively small $\lesssim 11 \text{ km}$ (Nicholl et al., 2017). If confirmed by additional modeling and numerical simulation work, this result would have key implications for the equation of state of the NS (e.g. Özel & Freire 2016).

The total mass of the red (lanthanide-bearing) ejecta was estimated to be $\approx 4 \times 10^{-2} M_\odot$ with a somewhat lower expansion velocity $v \approx 0.1 \text{ c}$ than the blue ejecta (e.g. Cowperthwaite et al. 2017; Chornock et al. 2017; Nicholl et al. 2017). Such a large quantity of ejecta, if originating from the tidal tail, would require an extremely asymmetric merger (e.g. Hotokezaka et al. 2013); however, this would not explain the low ejecta velocity, which based on numerical simulations is expected to be $\approx 0.2 - 0.3 \text{ c}$. Accretion disk winds provide a more natural explanation, as several $10^{-2} M_\odot$ expanding at $v \approx 0.1 \text{ c}$ matches theoretical expectations for the outflow from a massive torus $\gtrsim 0.1 M_\odot$ (e.g. Metzger, Piro & Quataert 2008; Fernández & Metzger 2013; Just et al. 2015; Wu et al. 2016; Siegel & Metzger 2017). A relatively spherical accretion disk outflow could be consistent with the non-detection of linear polarization from the late red kilonova emission (Covino et al., 2017).

Such a large torus is not expected if the merger event resulted in the prompt collapse to a BH, but instead suggests that at least a temporarily-stable hypermassive NS formed in GW170817 (e.g. Shibata & Taniguchi 2006). On the other hand, the fact that the disk outflows produced primarily ejecta with $Y_e \lesssim 0.25$ (as needed to power red kilonova emission) would, based on the results of numerical simulations of the disk evolution (Lippuner et al., 2017), implicate a relatively short hypermassive NS lifetime, $\lesssim 100 \text{ ms}$. This is consistent with the moderate inferred kinetic energy of the kilonova ejecta $\approx 10^{51} \text{ erg}$, which

does not require substantial additional energy input from the rotational energy of a temporarily-stable supramassive NS remnant (Metzger & Piro, 2014; Margalit & Metzger, 2017).

The kilonova emission from GW170817 probes the merger ejecta structure for one particular viewing angle and set of initial binary parameters. Future NS mergers observed from different viewing angles, or with a different total binary mass or binary asymmetry, could produce a quantitatively or qualitatively different signal. Some of these possibilities are described in the final take-aways section (§4).

How uncertain are the ejecta masses? Uncertainties enter estimates of the kilonova ejecta mass from at least three sources: geometry, the radioactive heating rate, and the thermalization efficiency of the decay products. While the thermalization efficiency of the early-time blue kilonova is relatively robust (Metzger et al., 2010), the total radioactive heating rate of $Y_e \gtrsim 0.25$ matter is uncertain at the factor of a few level (Lippuner & Roberts, 2015). By contrast, while for the red kilonova emission the total radioactive heating rate of $Y_e \lesssim 0.25$ matter is robust to within a factor $\lesssim 2$ (Metzger et al., 2010; Korobkin et al., 2012), the thermalization efficiency is less certain because it depends on the distribution of heating between β -decays, α -particle decay and fission (Barnes et al., 2016; Rosswog et al., 2017), which depend on the unknown masses of nuclei well off the valley of nuclear stability (Mendoza-Temis et al., 2015; Hotokezaka et al., 2015). Geometric effects also typically enter at the factor ≈ 2 level (Roberts et al., 2011; Grossman et al., 2014; Kasen et al., 2017). A reasonable guess is that the blue kilonova ejecta mass is accurate to a factor of $\approx 2 - 3$, but the red KN ejecta mass could be uncertain to a factor of $\approx 3 - 10$. Even given these uncertainties, and those on the overall rate of binary NS mergers, the discovery of GW170817 makes it likely that binary NS mergers are the dominant site of r -process nuclei in the universe (Lattimer & Schramm, 1974; Symbalisty & Schramm, 1982; Eichler et al., 1989; Freiburghaus et al., 1999).

3 A Gamma-Ray Burst and an Afterglow

GW170817 was accompanied by a short burst of gamma-rays (Goldstein et al. 2017; Savchenko et al. 2017; LIGO Scientific Collaboration et al. 2017b, dubbed GRB170817A), which was similar in duration to— but orders of magnitude less energetic than—standard cosmological short GRBs (see also Fong et al. 2017). The onset of GRB170817A was delayed by ≈ 1.7 seconds relative to the end of the merger, as inferred from the GW signal. This near temporal coincidence enabled constraints to be placed on fundamental physics, such as the difference between the speed of EM and gravitational waves (LIGO Scientific Collaboration et al., 2017b). Given the inference described above from the red kilonova emission that a massive accretion disk formed and that BH formation was relatively prompt in GW170817, such a torus-BH system provides a natural engine for powering a relativistic GRB jet (e.g. Narayan et al. 1992; Aloy et al. 2005).

GRB170817A was composed of two separate emission components, (1) an initial hard spike lasting $\lesssim 0.5$ seconds with a non-thermal spectrum broadly similar to normal short GRBs, followed by (2) a softer emission component lasting a few seconds with a spectrum consistent with being thermal (Goldstein et al. 2017; Savchenko et al. 2017). As discussed by LIGO Scientific Collaboration et al. (2017b), the first emission component could be the off-axis signature of a much more powerful short GRB jet, which either has its luminosity de-boosted by relativistic beaming or, alternatively, is “structured” in polar angle or time (e.g. Lamb & Kobayashi 2016; Kathirgamaraju et al. 2017). A thermal component could originate from the hot cocoon (Lazzati et al., 2017; Nakar & Piran, 2017) or shock break-out (Nakar & Sari, 2012) created as the ultra-relativistic GRB drills through the polar merger ejecta cloud (e.g. Duffell et al. 2015).

Temporal evolution of the jet’s structure is also natural. The post-merger accretion disk evolves on the viscous time of several seconds, over which time its mass is substantially depleted by accretion and outflows (e.g. Fernández & Metzger 2013; §2.1). If disk winds and the dynamical ejecta are the medium responsible for collimating the GRB jet then—as the density of the surrounding ejecta cloud and the jet power weaken in time—the jet opening angle may also widen on a timescale of a few seconds, similar to the observed delay of GRB170817A.¹

The possibility that GW170817 was viewed off-axis angle relative to the core of the GRB jet is consistent with the relatively large binary inclination angle relative to our line of site, $\theta_{\text{obs}} \approx 0.2 - 0.6$ (Table 1). The local rate of short GRBs viewed on-axis is $f_{\text{on}} \mathcal{R}_{\text{SGRB}} \approx 2 - 6 \text{ Gpc}^{-3} \text{ yr}^{-1}$ (Wanderman & Piran, 2015) is much less than the total GW-inferred rate of binary NS mergers $\mathcal{R}_{\text{BNS}} \approx 1540_{-1220}^{3200} \text{ Gpc}^{-3} \text{ yr}^{-1}$ (LIGO Scientific Collaboration & Virgo Collaboration, 2017a). Here $f_{\text{on}} \approx 0.3 - 1$ is the fraction of detected short GRBs which are observed on-axis; at a minimum this equals the $\approx 30\%$ of short GRBs with prompt and luminous X-ray afterglows detected by *Swift* that also enable the burst to be well-localized and the host galaxy to be identified to cosmological distances $z \sim 0.1 - 1$ (e.g. Fong et al. 2015). Assuming that every binary NS merger produces a short GRB, and that all short GRBs are binary NS mergers, the

¹Such evolution in the jet properties would not necessarily be expected in long duration GRBs because the outer mantle of the progenitor star responsible for jet collimation in this case does not evolve appreciably on the timescale of the burst.

implied beaming fraction $f_b \approx f_{\text{on}} \mathcal{R}_{\text{SGRB}} / \mathcal{R}_{\text{BNS}} \sim 1 \times 10^{-4} - 2 \times 10^{-2}$ and a corresponding half-opening angle for the core of the GRB jet of $\theta_j = (2f_b)^{1/2} \approx 0.02 - 0.2$. Thus, we infer that GW170817 was indeed most likely viewed outside the core of the jet, such that $\theta_{\text{obs}}/\theta_j \approx 1 - 30$ (see Fig. 4).

Additional evidence suggesting the presence of a more powerful off-axis jet is the discovery of non-thermal X-ray (Margutti et al., 2017; Troja et al., 2017) and radio emission (Hallinan et al., 2017; Murphy et al., 2017; Mooley et al., 2017; Alexander et al., 2017) following the merger with a delayed rise of several weeks. Such emission is naturally expected from an off-axis ‘‘orphan’’ GRB afterglow (e.g. Granot et al. 2002). At earlier times, the afterglow emission was relativistically beamed away from our line of site; however, as the GRB ejecta sweeps up gas from the ISM of the surrounding galaxy of density n , it begins to decelerate such that its Lorentz factor approaches a self-similar evolution with radius r (Blandford & McKee, 1976),

$$\Gamma = \left(\frac{17}{8\pi} \frac{E_j}{nm_p r^3 \theta_j^2 c^2} \right)^{1/2}, \quad (1)$$

where E_j is the total beaming-corrected energy of the jet. The initially de-beamed emission enters our causal cone, and the off-axis afterglow peaks, once $\Gamma \approx 1/\theta_{\text{obs}}$. Using the relationship between emission radius and observer time $t = r/(2\Gamma^2 c)$, this occurs on a timescale

$$t_{\text{pk}} \approx \left(\frac{17E_j}{64\pi nm_p c^5} \frac{\theta_{\text{obs}}^8}{\theta_j^2} \right)^{1/3} \approx 18 \text{ days} \left(\frac{n}{0.01 \text{ cm}^{-3}} \right)^{1/3} \left(\frac{E_j}{10^{50} \text{ erg}} \right)^{1/3} \left(\frac{\theta_{\text{obs}}}{5\theta_j} \right)^{2/3} \left(\frac{\theta_{\text{obs}}}{0.3} \right)^2, \quad (2)$$

where we have used the relationship between radius and the photon arrival time $t = r/(2\Gamma^2 c)$. Matching the estimated peak timescale of the X-ray and radio emission of $\approx 15 - 30$ days (e.g. Margutti et al. 2017; Troja et al. 2017; Hallinan et al. 2017; Alexander et al. 2017) suggests jet energies $E_j \sim 10^{49} - 10^{50}$ erg and ISM densities $n \sim 10^{-4} - 10^{-2} \text{ cm}^{-3}$ (e.g. Margutti et al. 2017; Alexander et al. 2017; Fong et al. 2017), broadly consistent with those inferred for on-axis short GRB (Nakar, 2007; Berger, 2014) and much less than those of star-forming environments which characterize long-duration GRBs.

Most of the $\approx 75\%$ of short GRBs discovered by *Swift* which are accompanied by luminous X-ray afterglows are presumably those events viewed on-axis, within or nearly within the opening angle of the jet, $\theta_{\text{obs}} \lesssim \theta_j$. However, it is interesting to ask what fraction of the remaining 25% could be off-axis dim nearby bursts similar to that observed from GW170817 and located at much closer distances $\approx 40 - 100$ Mpc (see also LIGO Scientific Collaboration et al. 2017b). The fraction of all mergers that would be viewed at the inferred inclination angle of GW170817 is $\approx (\theta_{\text{obs}}/\theta_j)^2 \sim 10 - 100$ times larger than the on-axis events. However, the isotropic fluence of the GRB associated with GW170817 of $E_{\text{iso}} \sim 4 \times 10^{46}$ erg (Goldstein et al., 2017) was $\sim 10^{2.5}$ times lower than the dimmest values for the cosmological short GRB population, in which case the detection volume is smaller by a factor of $\gtrsim 10^4$. Though crude, this estimate suggests that less than a few percent of the total short GRB population could arise from NS mergers as close as GW170817. A relatively nearby population (analogs of GW170817) appears to be broadly consistent with the inference by Tanvir et al. (2005) that $\approx 10 - 25\%$ of short GRBs originate from $\lesssim 70$ Mpc, based on a correlation between the sky position of BATSE short GRBs with local structure defined by catalogs of local galaxies.

4 Lessons Learned and Open Questions

Taking at face value the unified scenario for the multi-wavelength counterparts to GW170817 summarized by Fig. 2, I now recount what I believe are the major take-away lessons from the first binary NS merger GW170817 with EM follow-up. I address the question of how ‘‘typical’’ we should expect the EM signal from GW170817 to be, and, conversely, what counterpart diversity is expected as we move ahead to the era in which LIGO/Virgo approach design sensitivity and the NS mergers may be detected as frequently as once per week.

- **A triumph for theory.** While the detection of gamma-ray emission from an off-axis jet was surprising to many (however, see Lazzati et al. 2017), perhaps the biggest take-away from GW170817 is that theorists predicted the observed EM signals more or less accurately; the merger was surprisingly well-behaved. The discovery of both blue (Metzger et al., 2010) and red (Barnes & Kasen, 2013; Tanaka & Hotokezaka, 2013) kilonova emission was observed with the timescale, luminosity (indeed, ~ 1000 times brighter than a classical nova!), and colors predicted by theory (Fig. 1) for an ejecta mass and velocity consistent with those predicted by numerical simulations of the merger (e.g. Rosswog et al. 1999; Oechslin & Janka 2006; Sekiguchi et al. 2016) and the post-merger accretion flow (e.g. Fernández & Metzger 2013). Likewise, the prediction for an off-axis orphan afterglow, though not without degeneracies or free parameters, are broadly consistent with the observed non-thermal X-ray and radio emission for an observer situated at an angle relative to the binary axis

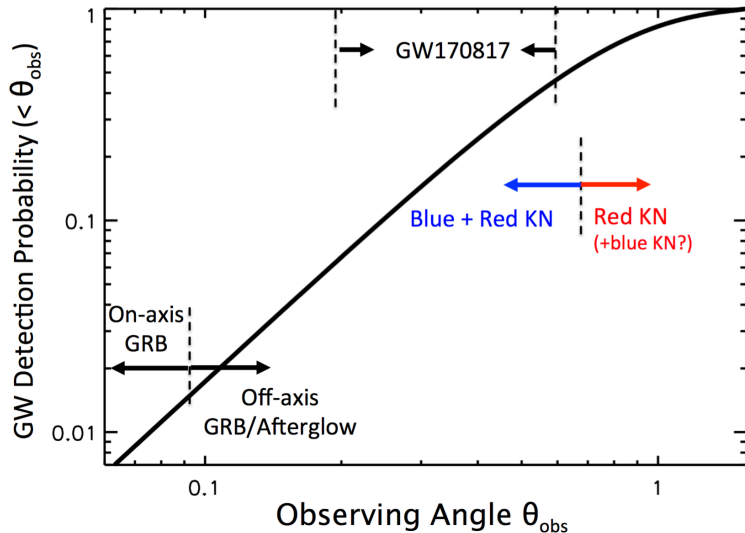


Figure 4: Probability of detecting GWs from a binary NS merger at an observing angle (as measured from the binary orbital axis) less than a value θ_{obs} from Schutz (2011). Shown for comparison are (1) the 1σ range of inclination angles inferred for GW170817 (when the degeneracy with distance is broken by the host galaxy distance; (LIGO Scientific Collaboration et al., 2017d)); (2) the approximate angle separating viewers within the lanthanide-free polar funnel of the dynamical ejecta (Sekiguchi et al., 2016), which observe both a blue and red kilonova signature, from those more equatorial viewers who might observe only the red kilonova component (if the blue kilonova is obscured); (3) the approximate angle $\theta_{\text{obs}} \lesssim \theta_j \approx 0.05 - 0.2$ separating mergers which produce on-axis cosmological short GRBs with prompt X-ray afterglows, from mergers viewed outside the jet axis who instead observe a weaker GRB and delayed orphan afterglow emission, as may have been observed in GW170817. Adapted from a similar figure in Margutti et al. (2017).

(Granot et al., 2002; van Eerten et al., 2010). This provides the most direct evidence yet that binary NS mergers are the source of most or all classical short GRBs observed at cosmological distances (e.g. Eichler, Livio, Piran & Schramm 1989).

- **An abundance of riches.** Given the significant quantity of r -process nuclei produced in GW170817, along with the relatively high implied merger rate, this strongly supports binary NS mergers as the dominant source of heavy r -process nuclei in the galaxy (e.g. Kasen et al. 2017; Cowperthwaite et al. 2017; Chornock et al. 2017; LIGO Scientific Collaboration & Virgo Collaboration 2017b), confirming long-standing theoretical ideas (Lattimer & Schramm, 1974; Symbalisty & Schramm, 1982; Eichler et al., 1989; Freiburghaus et al., 1999). The red kilonova emitting ejecta component dominates the total ejecta mass and thus likely also dominates the yield of both light and heavy r -process nuclei (Table 1). Assuming an r -process abundance pattern matching the solar one, one infers that over a hundred Earth masses in gold was created within a few seconds following GW170817.
- **Similar event, but different viewing angle?** GW170817’s relatively face-on orientation of $\theta_{\text{obs}} \approx 0.2 - 0.6$ will be shared by only $\approx 10 - 50\%$ of GW-discovered mergers (Fig. 4). For larger inclination angles, theory suggests the GRB and afterglow emission are unlikely to be sufficiently luminous to be detected, though observationally this is not yet well constrained (LIGO Scientific Collaboration et al. 2017b). The kilonova is predicted to be relatively isotropic (Roberts et al., 2011) and thus in principle should be visible with a similar luminosity (to within a factor of ≈ 2) for viewers observing the event closer to the binary plane. However, if the speed of the high-opacity lanthanide-rich equatorial tidal matter exceeds the speed of the blue polar ejecta, then the blue emission could be blocked or at least partially suppressed for the roughly half of the mergers viewed at $\theta_{\text{obs}} \gtrsim 0.6$ (Kasen, Fernández & Metzger, 2015). Although the average velocity of the red ejecta from GW170817 was inferred to be less than for the blue ejecta, even a small quantity $\lesssim 10^{-3}M_{\odot}$ of the lanthanide-rich matter moving at high velocities (which is challenging to rule out observationally) would be enough to at least partially attenuate the blue emission for less polar viewing angles. Much will be learned about the geometry of the kilonova ejecta from the luminosity of the early blue emission for the next NS merger observed at a higher inclination angle, closer to within the binary plane.
- **Similar event, but greater distance?** Luck may have played some role in the first NS merger discovery occurring at only 40 Mpc. For the same merger viewed at a distance more typical of those expected during LIGO/Virgo’s O3 science run next fall ($\gtrsim 100$ Mpc), the gamma-ray, X-ray and radio luminosities observed in GW170817 are probably too dim to be detected with current facilities. By contrast, the early blue kilonova observed on timescales of $\lesssim 1$ day would still reach a visual magnitude of $R = 19.5$ at 100 Mpc or $R = 21$ at 200 Mpc, within the reach of moderate-sized wide-field follow-up telescopes, such as the Zwicky Transient Facility (Bellm, 2014) and the BlackGEM array (Bloemen et al., 2016). Even kilonovae for which the early blue emission is blocked or suppressed would be detectable to 200 Mpc distances by more sensitive telescopes such as DECam (Cowperthwaite et al. 2017b). With a magnitude depth of $R = 25 - 26$, the Large Synoptic Survey

Telescope (LSST) could detect a similar blue kilonova to distances $\gtrsim 1$ Gpc! Kilonovae still represent the counterpart most likely to accompany the majority of mergers (Metzger & Berger, 2012).

- **Similar event, but greater binary mass?** The large quantity of ejecta from GW170817 suggests that a temporarily stable hypermassive NS remnant was created during the merger. The total binary mass $\approx 2.3 - 2.78M_{\odot}$ (Table 1, assuming low NS spin) is broadly consistent with that expected by drawing two stars from the the Galactic NS population (well-described by a Gaussian of mean $\mu = 1.32M_{\odot}$ and standard deviation $\sigma = 0.11M_{\odot}$; Kiziltan et al. 2013). For more massive binaries (with precisely how massive—and thus how rare—depending sensitively on the maximum NS mass), a prompt collapse would occur instead of the formation of a hypermassive NS. In such a case the blue kilonova would be strongly suppressed, especially the polar dynamical component. The red kilonova also might now be dominated by the tidal tail ejecta instead of the disk outflows and thus would also be somewhat dimmer. All else being equal (e.g. similar observing inclination), an inverse relationship is expected between the kilonova luminosity and the total binary mass.
- **Similar event, but lower binary mass?** For less massive binaries, a long-lived supramassive or stable NS remnant could form instead of a short-lived hypermassive NS (e.g. Özel et al. 2010; Piro et al. 2017). In such cases, a fraction of the substantial rotational energy of the remnant (communicated, e.g., by magnetic spin-down) is likely to be transferred to the kilonova ejecta (Bucciantini et al., 2012), accelerating it to higher speeds $v \sim c$ than inferred for GW170817. This additional source of acceleration and rotational energy input may power a signal with an optical and X-ray luminosity much higher than what is possible from r -process heating alone (Yu et al., 2013; Metzger & Piro, 2014; Siegel & Ciolfi, 2016) and a faster evolution timescale. An ultra-relativistic outflow from a long-lived remnant may also power the mysterious variable X-ray/gamma-ray emission observed for hundreds or thousands of seconds following some short GRBs (Norris & Bonnell, 2006; Rowlinson et al., 2013). No evidence for such “extended emission” was observed at hard X-ray/gamma-ray energies following GW170817 (LIGO Scientific Collaboration et al., 2017b). Still, it would not be surprisingly to see qualitatively different EM behavior from the low mass tail of the NS binary merger population.
- **BH-NS instead of NS-NS?** What if GW170817 had been the merger between a NS and a stellar mass BH instead of a NS-NS? If GW170817’s blue kilonova was indeed the result of matter squeezed out of the polar region by the colliding NSs, then a similar component of fast high- Y_e ejecta and its concomitant blue kilonova emission will not be present for BH-NS mergers. If the mass of the BH is sufficiently low, and/or its spin sufficiently high, to disrupt the NS outside of the BH innermost stable circular orbit, then the tidal ejecta mass is typically $\sim 0.1M_{\odot}$ (Foucart, 2012), much higher than that in NS-NS mergers. Although this is consistent with the higher red ejecta mass inferred for GW170817, the average velocity of the tidal ejecta from a NS-BH will be higher, closer to $\approx 0.2 - 0.3 c$, than inferred for GW170817. A disrupted NS will also produce a massive accretion torus as in the NS-NS case, potentially capable of powering a GRB jet. A moderate quantity of blue kilonova ejecta from the accretion disk outflows are expected in this case (e.g. Fernández et al. (2017) finds $\lesssim 8 \times 10^{-3}M_{\odot}$ in $Y_e \gtrsim 0.25$ disk wind ejecta; Kyutoku et al. 2017). Again, however, the velocity of the disk outflow is predicted to be lower $\lesssim 0.1 c$ than that inferred for GW170817, and it may be blocked by the tidal ejecta for equatorial viewers.
- **Implications for the radii of NSs.** The inference of a small NS radius $\lesssim 11$ km (e.g. Nicholl et al. 2017) would have critical implications for the equation of state (Özel & Freire, 2016). This conclusion is predicated on the large quantity $\approx 10^{-2}M_{\odot}$ of blue kilonova ejecta inferred from GW170817 being the result of dynamical ejecta produced by the merger collision, as opposed to outflows from the post-merger accretion disk. This hypothesis could potentially be checked by searching for similar early blue emission from future NS-NS mergers seen from a similar binary inclination. The polar dynamical ejecta should be quantitatively similar between NSs of moderately different masses (the radius of a NS is almost independent of its mass for typical masses). However, the disk outflows should vary more strongly with the total mass of the system and the asymmetry of the binary. Thus, if the early blue emission of the type observed in GW170817 is observed with very similar properties for a range of binaries with different masses (and otherwise similar polar viewing angles), this would favor it being dynamical in origin and thus the hypothesis of a small NS radius. Additional numerical work, with better neutrino transport and resolution at the collision interface between the NSs, are also needed to solidify the use of kilonovae as probes of the NS radius.
- **Implications for the maximum NS mass.** The lack of evidence for either a prompt collapse (from the large inferred quantity of kilonova ejecta) or the formation of a supramassive NS remnant (from the prompt GRB and moderate kinetic energy of the kilonova ejecta) points to the formation of a hypermassive NS remnant in GW170817. Using a suite of representative NS equations of state, the gravitational masses of the NS-NS binary measured by Advanced LIGO/Virgo can be used to

place an upper limit on the maximum stable mass of a slowly-rotating NS of $M_{\max} \lesssim 2.17M_{\odot}$ at 90% confidence (Margalit & Metzger, 2017). This upper limit on M_{\max} is tighter, and arguably less model-dependent, than other observational or theoretical constraints. This constraint would be strengthened or tightened with the discovery of additional mergers, particularly if the lowest-mass binaries also show no evidence for a supramassive NS remnant.

- **Implications for merger cosmology.** The EM follow-up campaign of GW170817 demonstrates a proven method to obtain a redshift for a GW event, thus opening the potential of binary NS merger as “standard sirens” to study the expansion history of the universe (Schutz, 1986; Holz & Hughes, 2005). A comparison of the luminosity distance from the GW signal of GW170817 with the measured redshift of the host galaxy led to a measurement of the Hubble constant of $H_0 = 69.3^{12.1}_{-6.0}$ km s⁻¹ Mpc⁻¹ which is completely independent of, and fully consistent with, other estimates of H_0 (LIGO Scientific Collaboration et al., 2017d). The GW detection rate of binary NS mergers will reach 6–120 per year once Advanced LIGO/Virgo reach design sensitivity (LIGO Scientific Collaboration & Virgo Collaboration, 2017a). A larger sample of GW+redshift events, enabled by kilonova observations, will place increasingly tight constraints on H_0 (Nissanke et al., 2010). As knowledge of the angular structure of short GRB jets grows, increasingly realistic priors on the binary inclination may enable the subset of events with detected GRBs of a given luminosity to play an outsized role in the analysis.

Looking ahead to decade timescales, as additional GW detectors like KAGRA (Aso et al., 2013) and LIGO India enter the network and if the Advanced LIGO detectors are upgraded (e.g. to the so-called “A+” enhanced configuration), then horizon distance approaching $\approx 0.7 - 2$ Gpc (redshift $z \approx 0.1 - 0.4$) may be achievable for NS-NS and NS-BH mergers, respectively. At the latter distances the sample of events with on-axis GRBs also becomes substantial (e.g. LIGO Scientific Collaboration et al. 2017b) and detecting the blue kilonova counterparts, while still possible, would require a telescope with higher sensitivity like LSST. Once redshifts $z \gtrsim 0.4$ become accessible, GW/EM sirens from NS mergers (particularly the subset of NS-BH mergers with kilonovae and short GRBs) could provide an alternative method to probe additional cosmological parameters such as Dark Energy in a way complimentary to existing methods (e.g. Ia SNe, Baryon Acoustic Oscillations), but independent of the cosmic distance ladder.

Acknowledgements

This summary is dedicated to Alastair (Al) Cameron (1925-2005). Cameron discovered the r -process in 1957 contemporaneously with B²FH and deciphering its astrophysical origin remained a passion throughout his career. One of Al’s last publications, around the time I entered graduate school, hypothesized an r -process origin in magnetized jets from compact object accretion disks created in core collapse supernovae (Cameron, 2003). Similar magnetized outflows from the post-merger accretion disk (e.g. Siegel & Metzger 2017) may have provided the dominant source of the heavy r -process inferred from the kilonova emission in GW170817 and thus (as far as we can presently discern) the universe as a whole. I thank Gabriel Martinez-Pinedo for comments on this draft. I also thank all of my observational collaborators in the DECAM GW follow-up team. BDM was supported in part by NASA grant NNX16AB30G.

References

- Alexander K. D., et al., 2017, ApJL in press
- Allam S., et al., 2017, GCN, 21530, 1
- Aloy M. A., Janka H.-T., Müller E., 2005, A&A, 436, 273
- ANTARES IceCube LVC et al., 2017, ApJL
- Arcavi I., et al., 2017a, ApJL
- Arcavi I., et al., 2017b, Nature
- Arnould M., Goriely S., Takahashi K., 2007, Phys. Rep., 450, 97
- Aso Y., Michimura Y., Somiya K., Ando M., Miyakawa O., Sekiguchi T., Tatsumi D., Yamamoto H., 2013, Phys. Rev. D., 88, 043007
- Barnes J., Kasen D., 2013, ApJ, 775, 18

Barnes J., Kasen D., Wu M.-R., Mart'inez-Pinedo G., 2016, ArXiv e-prints

Bauswein A., Baumgarte T. W., Janka H.-T., 2013, Physical Review Letters, 111, 131101

Bauswein A., Goriely S., Janka H.-T., 2013, ApJ, 773, 78

Bellm E., 2014, in Wozniak P. R., Graham M. J., Mahabal A. A., Seaman R., eds, The Third Hot-wiring the Transient Universe Workshop The Zwicky Transient Facility. pp 27–33

Berger E., 2014, ARA&A, 52, 43

Berger E., et al., 2005, Nature, 438, 988

Blandford R. D., McKee C. F., 1976, Physics of Fluids, 19, 1130

Bloemen S., et al., 2016, in Ground-based and Airborne Telescopes VI Vol. 9906 of Procspie, MeerLICHT and BlackGEM: custom-built telescopes to detect faint optical transients. p. 990664

Bloom J. S., et al., 2006, ApJ, 638, 354

Bloom J. S., et al., 2009, ApJ, 691, 723

Bucciantini N., Metzger B. D., Thompson T. A., Quataert E., 2012, MNRAS, 419, 1537

Burbidge E. M., Burbidge G. R., Fowler W. A., Hoyle F., 1957, Rev. Mod. Phys., 29, 547

Cameron A. G. W., 1957, PASP, 69, 201

Cameron A. G. W., 2003, ApJ, 587, 327

Chornock R., et al., 2017, ApJL accepted

Coulter D. A., et al., 2017, Science

Covino S., et al., 2017, nature Astronomy

Cowperthwaite P., et al., 2017, ApJL

Cowperthwaite P. S., Berger E., Rest A., Chornock R., Scolnic D. M., Williams P. K. G., Fong W., Drout M. R., Foley R. J., Margutti R., Lunnan R., Metzger B. D., Quataert E., 2017, ArXiv e-prints

Davies M. B., Benz W., Piran T., Thielemann F. K., 1994, ApJ, 431, 742

Dessart L., Ott C. D., Burrows A., Rosswog S., Livne E., 2009, ApJ, 690, 1681

Duffell P. C., Quataert E., MacFadyen A. I., 2015, ApJ, 813, 64

Eichler D., Livio M., Piran T., Schramm D. N., 1989, Nature, 340, 126

Evans P., Cenko S., Kennea J., et al., 2017, Science

Fernández R., Foucart F., Kasen D., Lippuner J., Desai D., Roberts L. F., 2017, Classical and Quantum Gravity, 34, 154001

Fernández R., Metzger B. D., 2013, MNRAS, 435, 502

Fernández R., Metzger B. D., 2016, Annual Review of Nuclear and Particle Science, 66, 23

Fernández R., Quataert E., Schwab J., Kasen D., Rosswog S., 2015, MNRAS, 449, 390

Fong W., Berger E., Margutti R., Zauderer B. A., 2015, ApJ, 815, 102

Fong W., et al., 2017, ApJL accepted

Foucart F., 2012, PRD, 86, 124007

Fox D. B., et al., 2005, Nature, 437, 845

Freiburghaus C., Rosswog S., Thielemann F., 1999, ApJ, 525, L121

Goldstein A., et al., 2017, ApJL, 848

Goriely S., Bauswein A., Janka H.-T., 2011, *ApJ*, 738, L32

Goriely S., Bauswein A., Just O., Pllumbi E., Janka H.-T., 2015, *MNRAS*, 452, 3894

Granot J., Panaitescu A., Kumar P., Woosley S. E., 2002, *ApJL*, 570, L61

Grossman D., Korobkin O., Rosswog S., Piran T., 2014, *MNRAS*, 439, 757

Haggard D., et al., 2017, *ApJL*

Hallinan G., Corsi A., et al., 2017, submitted

Hjorth J., Watson D., Fynbo J. P. U., Price P. A., Jensen B. L., Jørgensen U. G., Kubas D., Gorosabel J., Jakobsson P., Sollerman J., Pedersen K., Kouveliotou C., 2005, *Nature*, 437, 859

Holz D. E., Hughes S. A., 2005, *ApJ*, 629, 15

Hotokezaka K., Kiuchi K., Kyutoku K., Okawa H., Sekiguchi Y.-I., Shibata M., Taniguchi K., 2013, *Phys. Rev. D*, 87, 024001

Hotokezaka K., Piran T., Paul M., 2015, *Nature Physics*, 11, 1042

Hotokezaka K., Sari R., Piran T., 2017, *MNRAS*, 468, 91

Ji A. P., Frebel A., Chiti A., Simon J. D., 2016, *Nature*, 531, 610

Just O., Bauswein A., Pulpillo R. A., Goriely S., Janka H.-T., 2015, *MNRAS*, 448, 541

Kasen D., Badnell N. R., Barnes J., 2013, *ApJ*, submitted, arXiv:1303.5788

Kasen D., Fernández R., Metzger B. D., 2015, *MNRAS*, 450, 1777

Kasen D., Metzger B., Barnes J., Ramirez-Ruiz Quataert E., 2017, *Nature*

Kasliwal M., et al., 2017, *Science*, 21530

Kasliwal M. M., Nissanke S., 2014, *ApJL*, 789, L5

Kathirgamaraju A., Barniol Duran R., Giannios D., 2017, *ArXiv e-prints*

Kilpatrick C., et al., 2017, *Science*

Kiziltan B., Kottas A., De Yoreo M., Thorsett S. E., 2013, *ApJ*, 778, 66

Korobkin O., Rosswog S., Arcones A., Winteler C., 2012, *MNRAS*, 426, 1940

Kyutoku K., Kiuchi K., Sekiguchi Y., Shibata M., Taniguchi K., 2017, *ArXiv e-prints*

Lamb G. P., Kobayashi S., 2016, *ArXiv e-prints*

Lattimer J. M., Mackie F., Ravenhall D. G., Schramm D. N., 1977, *ApJ*, 213, 225

Lattimer J. M., Schramm D. N., 1974, *ApJL*, 192, L145

Lazzati D., Deich A., Morsony B. J., Workman J. C., 2017, *MNRAS*, 471, 1652

Levan A., Tanvir N., 2017, *ApJL*

Li L., Paczyński B., 1998, *ApJ*, 507, L59

LIGO Scientific Collaboration Virgo Collaboration 2017a, *PhRvL*, 119

LIGO Scientific Collaboration Virgo Collaboration 2017b, *ApJL*

LIGO Scientific Collaboration Virgo Collaboration et al., 2017a, *ApJL*

LIGO Scientific Collaboration Virgo Collaboration et al., 2017b, *ApJL*

LIGO Scientific Collaboration Virgo Collaboration et al., 2017c, *PhRVL*

LIGO Scientific Collaboration Virgo Collaboration et al., 2017d, *Nature* submitted

Lippuner J., Fernández R., Roberts L. F., Foucart F., Kasen D., Metzger B. D., Ott C. D., 2017, MNRAS, 472, 904

Lippuner J., Roberts L. F., 2015, ArXiv e-prints

Lipunov V., et al., 2017, GCN, 21546, 1

Macias P., Ramirez-Ruiz E., 2016, ArXiv e-prints

Margalit B., Metzger B. D., 2017, PhRvL submitted

Margutti M., et al., 2017, ApJL accepted

Martin D., Perego A., Arcones A., Thielemann F.-K., Korobkin O., Rosswog S., 2015, ApJ, 813, 2

McCully C., et al., 2017, ApJL

Mendoza-Temis J. d. J., Wu M.-R., Langanke K., Martínez-Pinedo G., Bauswein A., Janka H.-T., 2015, PRC, 92, 055805

Metzger B. D., 2017, Living Reviews in Relativity, 20, 3

Metzger B. D., Berger E., 2012, ApJ, 746, 48

Metzger B. D., Fernández R., 2014, MNRAS, 441, 3444

Metzger B. D., Martínez-Pinedo G., Darbha S., Quataert E., Arcones A., Kasen D., Thomas R., Nugent P., Panov I. V., Zinner N. T., 2010, MNRAS, 406, 2650

Metzger B. D., Piro A. L., 2014, MNRAS, 439, 3916

Metzger B. D., Piro A. L., Quataert E., 2008, MNRAS, 390, 781

Meyer B. S., 1989, ApJ, 343, 254

Mooley K. P., et al., 2017, GCN, 21814, 1

Murphy T., et al., 2017, GCN, 21842, 1

Nakar E., 2007, PhysRep, 442, 166

Nakar E., Piran T., 2017, ApJ, 834, 28

Nakar E., Sari R., 2012, ApJ, 747, 88

Narayan R., Paczynski B., Piran T., 1992, ApJ, 395, L83

Nicholl N., et al., 2017, ApJL in press

Nissanke S., Holz D. E., Hughes S. A., Dalal N., Sievers J. L., 2010, ApJ, 725, 496

Norris J. P., Bonnell J. T., 2006, ApJ, 643, 266

Oechslin R., Janka H.-T., 2006, MNRAS, 368, 1489

Özel F., Freire P., 2016, ARA&A, 54, 401

Özel F., Psaltis D., Ransom S., Demorest P., Alford M., 2010, ApJL, 724, L199

Perego A., Rosswog S., Cabezón R. M., Korobkin O., Käppeli R., Arcones A., Liebendörfer M., 2014, MNRAS, 443, 3134

Pian E., et al., 2017, Science

Piran T., Nakar E., Rosswog S., 2013, MNRAS, 430, 2121

Piro A. L., Giacomazzo B., Perna R., 2017, ApJL, 844, L19

Qian Y., Woosley S. E., 1996, ApJ, 471, 331

Radice D., Galeazzi F., Lippuner J., Roberts L. F., Ott C. D., Rezzolla L., 2016, MNRAS, 460, 3255

Roberts L. F., Kasen D., Lee W. H., Ramirez-Ruiz E., 2011, *ApJL*, 736, L21

Rosswog S., 2015, *International Journal of Modern Physics D*, 24, 30012

Rosswog S., Feindt U., Korobkin O., Wu M.-R., Sollerman J., Goobar A., Martinez-Pinedo G., 2017, *Classical and Quantum Gravity*, 34, 104001

Rosswog S., Liebendörfer M., Thielemann F., Davies M. B., Benz W., Piran T., 1999, *A&A*, 341, 499

Rowlinson A., O'Brien P. T., Metzger B. D., Tanvir N. R., Levan A. J., 2013, *MNRAS*, 430, 1061

Ruffert M., Janka H.-T., Takahashi K., Schaefer G., 1997, *A&A*, 319, 122

Savchenko A., et al., 2017

Schutz B. F., 1986, *Nature*, 323, 310

Schutz B. F., 2011, *Classical and Quantum Gravity*, 28, 125023

Sekiguchi Y., Kiuchi K., Kyutoku K., Shibata M., Taniguchi K., 2016, *Phys. Rev. D*, 93, 124046

Shappee B., et al., 2017, *Science*

Shibata M., Taniguchi K., 2006, *Phys. Rev. D*, 73, 064027

Siegel D. M., Ciolfi R., 2016, *ApJ*, 819, 14

Siegel D. M., Metzger B. D., 2017, *ArXiv e-prints*

Smartt S., et al., 2017, *Nature*

Soares-Santos M., et al., 2017, *ApJL*, 21686, 1

Symbalisty E., Schramm D. N., 1982, *ApJL*, 22, 143

Tanaka M., Hotokezaka K., 2013, *ApJ*, 775, 113

Tanaka M., Kato D., Gaigalas G., Rynkun P., Radziute L., Wanajo S., Sekiguchi Y., Nakamura N., Tanuma H., Murakami I., Sakaue H. A., 2017, *ArXiv e-prints*

Tanvir N., Levan A., 2017, *ApJL*, 21530, 1

Tanvir N. R., Chapman R., Levan A. J., Priddey R. S., 2005, *Nature*, 438, 991

Troja E., Piro L., van Eerten H., et al., 2017, *Nature*

van Eerten H., Zhang W., MacFadyen A., 2010, *ApJ*, 722, 235

Verrechia V., et al., 2017, *MNRAS Letters*

Wallner A., Faestermann T., Feige J., Feldstein C., Knie K., Korschinek G., Kutschera W., Ofan A., Paul M., Quinto F., Rugel G., Steier P., 2015, *Nature Communications*, 6, 5956

Wanajo S., Sekiguchi Y., Nishimura N., Kiuchi K., Kyutoku K., Shibata M., 2014, *ApJL*, 789, L39

Wanderman D., Piran T., 2015, *MNRAS*, 448, 3026

Wollaeger R. T., Korobkin O., Fontes C. J., Rosswog S. K., Even W. P., Fryer C. L., Sollerman J., Hungerford A. L., van Rossum D. R., Wollaber A. B., 2017, *ArXiv e-prints*

Wu M.-R., Fernández R., Martínez-Pinedo G., Metzger B. D., 2016, *MNRAS*, 463, 2323

Yang S., et al., 2017, *GCN*, 21531, 1

Yu Y.-W., Zhang B., Gao H., 2013, *ApJL*, 776, L40